Available online at www.sciencedirect.com

ScienceDirect

Ceramics International 35 (2009) 3321–3325

CERAMICS INTERNATIONAL

www.elsevier.com/locate/ceramint

# Photocatalytic activity of transparent porous glass supported $TiO_2$

Tetsuo Yazawa [a,*], Fumiko Machida [a], Noriaki Kubo [b], Tetsuro Jin [c]

[a] *Graduate School of Engineering, University of Hyogo, 2167 Shosha, Himeji, Hyogo 671-2201, Japan*
[b] *Nihon Hels Industry Company, Shinjyuku, Tokyo 162-0813, Japan*
[c] *National Institute of Advanced Industrial Science & Technology (AIST), 1-8-31 Midorigaoka, Ikeda, Osaka 563-8577, Japan*

Received 6 April 2009; received in revised form 23 April 2009; accepted 24 May 2009
Available online 18 June 2009

## Abstract

A porous glass tube with a composition of $96SiO_2 \cdot 4B_2O_3$ (wt%) supported $TiO_2$ shows high photooxidation activity due to its transparency and large surface area. The surface area of the porous glass tube supported $TiO_2$ is 10,000 times larger than that of conventional materials. $TiO_2$ crystals supported are anatase type. Transparency of the porous glass tube is very important. Herein, sol–gel and chemical vapor deposition (CVD) processes were employed as $TiO_2$ supporting processes. CVD process is more effective. For instance, an aqueous methylene blue solution with 1 ppm concentration almost thoroughly decomposes at a contact time of 300 s using porous glass tube supported $TiO_2$ prepared by CVD process under irradiating with 10 W low-pressure mercury lamp, on the other hand, opaque porous alumina tube supported $TiO_2$ was only 25%. The smaller the pore size of the porous glass tube, the larger the transparency and the permeation resistance through porous glass tube. Hence, porous glass tube with ca. 40 nm pore diameter is suitable from the standpoint of a practical use.

*Keywords:* A. Sol–gel process; D. Glass; D. $TiO_2$; D. Silicate

## 1. Introduction

Titanium oxide ($TiO_2$) has been widely used as an effective photocatalyst because of its appropriate band gap energies of approximately 3.0 eV, thermal/chemical stabilities as well as its low fabrication cost [1]. Various types of $TiO_2$ such as powders, coating films or composites with heterointerfaces have been studied so far [2–5]. Among them, adsorbents modified with $TiO_2$ have attracted much attention since they can be used for applications to air- and/or water-purification, antifouling protection and bleaching, etc. [6,7]. Conventionally, the photocatalysts are used in dispersed form and are very difficult to collect after use. To overcome this shortcoming, photocatalysts have recently been developed in which $TiO_2$ was coated on appropriate substrates, such as a ceramic, glass or metal plate, or glass tube, by sol–gel process [8–11]. In these applications, the coated $TiO_2$ easily peels off from the substrate. Recently, in order to solve this, a novel porous $TiO_2$ glass-ceramics with high photocatalytic activity was prepared in the $SiO_2$–$Al_2O_3$–$B_2O_3$–CaO–$TiO_2$ glass system by the crystallized glass process [12], however, this glass-ceramics was opaque.

To enhance the photoreaction, it is important to enlarge the surface area of $TiO_2$. If $TiO_2$ is supported on the pore surface of transparent porous materials such as porous glass, a very large surface area can be used as a photoreaction field. The key concept of this paper is indicated in Fig. 1. The surface area often increases over $10^5$ times compared to the conventional materials. Furthermore, porous glass can concentrate the reacting species on its pore surface. As well, porous glass can be easily shaped into sheets, tubes, rods, etc. Consequently, porous glass is highly suitable for incorporation into a photocatalytic reactor. This paper describes the preparation of a transparent porous glass supported $TiO_2$ and its photocatalytic activity.

## 2. Experimental procedure

### 2.1. Preparation of the porous glass

In this experiment, porous glass with a composition of $SiO_2$ 96 and $B_2O_3$ 4 (wt%) was employed. This porous glass was

---

* Corresponding author at: Graduate School of Engineering, Department of Materials and Chemistry, University of Hyogo, 2167 Shosha, Himeji, Hyogo 671-2201, Japan. Tel.: +81 79 267 4896; fax: +81 79 267 4896.
*E-mail address:* yazawa@eng.u-hyogo.ac.jp (T. Yazawa).

0272-8842/$36.00 © 2009 Elsevier Ltd and Techna Group S.r.l. All rights reserved.
doi:10.1016/j.ceramint.2009.05.029

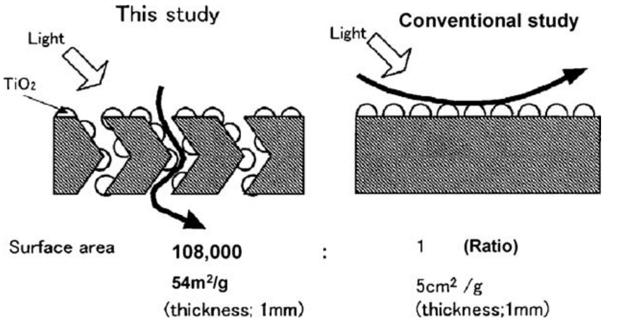

Fig. 1. Features of photooxidation by supported $TiO_2$ porous glass tube.

prepared by acid leaching after phase separation of sodium borosilicate glass with a composition of $SiO_2$ 62.4, $B_2O_3$ 28.3 and $Na_2O$ 9.3 (wt%) [13–15]. The heat treatment for phase separation was ranged from 570 to 600 °C and from 32 to 70 h, respectively. The porous glass was shaped into a tube with outer diameter of 5 mm and inner one of 4 mm. For the transparency measurements, a plate-type glass with 3 $mm^2$ and 0.5 mm thick was prepared.

### 2.2. $TiO_2$ supporting process

Two supporting processes were employed. One was sol–gel process and the other was chemical vapor deposition (CVD) process. Sol–gel process was performed as follows. The porous glass was impregnated in titanium tetraisopropoxide/methanol solution at a concentration of 50 wt% for 10 h and subsequently hydrolyzed by 0.1N aqueous $HNO_3$ solution. CVD process was conducted as follows. Fig. 2 shows the experimental apparatus. Vapor of titanium tetraisopropoxide ($Ti(O^iC_3H_7)_4$) was afforded into the electric furnace by bubbling of dry $N_2$ gas as a carrier gas and dry $O_2$ gas as an oxidizing agent. The porous glass tube was situated inside the furnace and the inner side of the tube was kept at a reduced pressure. The temperature of the furnace was maintained at 300 °C for 2.5 h. Regardless of the processes, the porous glass supported $TiO_2$ was calcinated at 550 °C for 15 h.

### 2.3. Characterization

Crystalline phase of the supported $TiO_2$ was analyzed by X-ray diffraction (XRD) measurements with Cu Kα radiation (Mini Flex Rigaku Co.). Specific surface area, pore volume and pore size of the samples were calculated from $N_2$ adsorption–desorption isotherms at 77 K (Belsorp mini, Bel Japan, Inc.).

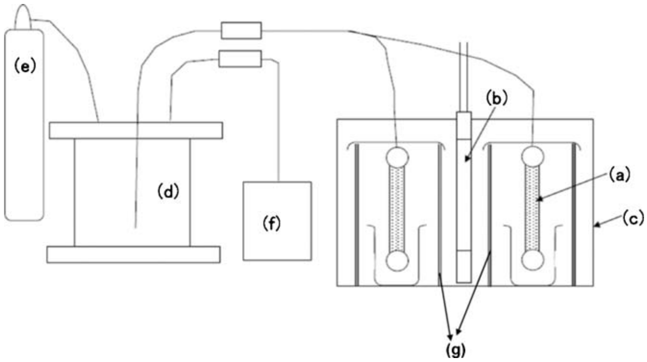

Fig. 3. Evaluation apparatus for photooxidation: (a) porous glass tube supported $TiO_2$, (b) low-pressure mercury lamp, (c) mirror, (d) feed solution, (e) $N_2$ gas cylinder, (f) pressure gauge and (g) quartz glass cell.

Samples were heated at 250 °C in vacuum in order to remove the adsorbed water in pores prior to the measurement. The pore size distribution was determined by the Barrett–Joyner–Halenda (BJH) method [16]. In case of pore size larger than 40 nm, mercury porosimetry (Pore Sizer 9310, Micromeritics Co.) was used.

### 2.4. Measurement of water flux

Water flux was measured by weighting of water through porous glass tube within the prescribed time interval under the prescribed pressure by $N_2$ cylinder.

### 2.5. Evaluation of photooxidation

The evaluation apparatus is shown in Fig. 3. The feed solution was an aqueous methylene blue solution with concentration from 0.4 to 10 ppm. The solution was afforded by the pressure of $N_2$ cylinder. The irradiation lamp was 10 W low-pressure mercury lamp (Sen Tokushu Kogen Co.). The length of the glass tube was 10 cm.

## 3. Results and discussion

### 3.1. Relationship between the transparency and pore size of porous glass

Fig. 4 shows the pore size distributions of the porous glass tubes A, B and C and Table 1 indicates the preparation conditions and pore characteristics. Fig. 5 shows the relationship between the transparency and pore size of the porous glass

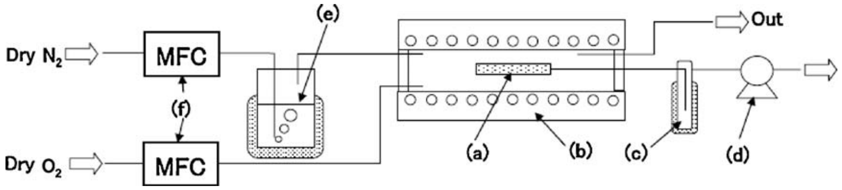

Fig. 2. Apparatus for CVD process: (a) porous glass tube, (b) electric furnace, (c) cold trap, (d) rotary pump, (e) $Ti(OC_3H_7)_4$ bubbler with thermostat and (f) mass flow controller.

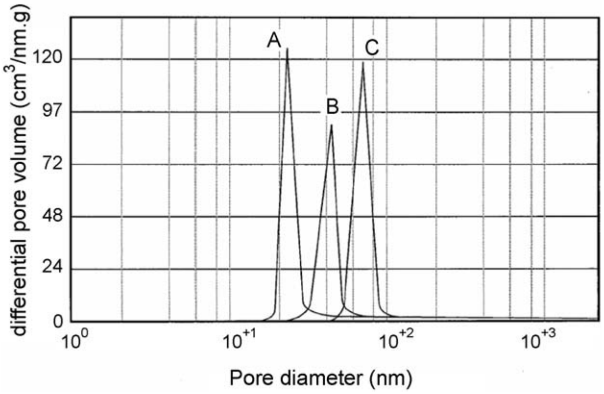

Fig. 4. Pore size distribution of the porous glass tubes A, B and C.

Table 1
Preparation conditions and pore characteristics of porous glass tubes.

| Porous glass tube | Condition | | Surface area/$m^2\ g^{-1}$ | Pore volume/$cm^3\ g^{-1}$ |
|---|---|---|---|---|
| | Temperature/°C | Time/h | | |
| A | 570 | 32 | 129 | 0.79 |
| B | 600 | 32 | 54 | 0.51 |
| C | 600 | 70 | 47 | 0.77 |

tube. The smaller the pore size, the larger the transparency due to the scattering on the pore surface. This scattering is considered to be Rayleigh scattering since the pore size is about one-tenth of the wavelength of the employed light. Rayleigh scattering is expressed as follows [17]:

$$I \propto \lambda^{-4} A, \quad A = \left[\frac{{n_1}^2 - n^2}{{n_1}^2 + 2n^2}\right]^2$$

where $I$ is the intensity of scattering, $n$ is the refractive index of medium, $n_1$ is the refractive index of the particle, and $\lambda$ is the wavelength of light. In case of scattering in air, $n = 1.0$ and $n_1 = 1.5$ (the refractive index of glass), $A$ of 0.08 is obtained. On the other hand, in case of soaking in water, $n = 1.33$ (refractive index of water) and $n_1 = 1.5$, $A$ of 0.007 is calculated. This indicates that the intensity of scattering while soaking in water is about one-tenth as weak as that in air. Consequently, in water, scattering is eminently decreased.

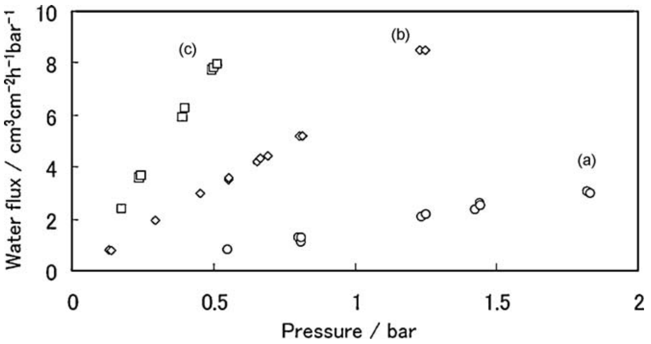

Fig. 6. Effect of pore size of the porous glass tubes on water flux: (a) porous glass tube A, (b) porous glass tube B and (c) porous glass tube C.

### 3.2. Relationship between the permeation resistance of water and the pore size of porous glass

Fig. 6 shows the water flux through the porous glass tube. It is clear the flux obeys the following Poiseuille flow [18].

$$Q \propto d^2$$

where $Q$ is the water flux and $d$ is the pore diameter. Thus, the flux is proportional to the square of the pore size. On the other hand, the transparency is related to the pore size as shown in Fig. 5. Hence, adjusting the transparency and flux is very important. In this paper, porous glass tube B was employed at the standpoint of a practical use.

### 3.3. Transparency of the porous glass supported $TiO_2$

Fig. 7 shows the relationship between the number of impregnation and the transparency. The transparency derived from sol–gel process depends on the number of impregnation. The fewer the number of impregnation, the larger the transparency. Transparency after CVD is also indicated in

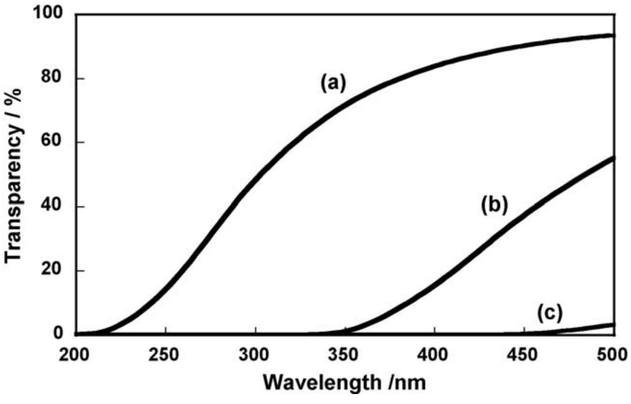

Fig. 5. Effect of pore size of the porous glass tubes on transparency, thickness = 5 mm: (a) porous glass plate A, (b) porous glass plate B and (c) porous glass plate C.

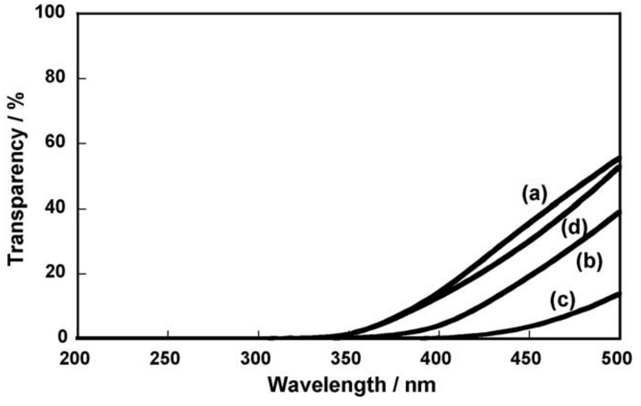

Fig. 7. Effect of the impregnation number on transparency by sol–gel process with porous glass tube B: (a) without any treatment, (b) 1 time, (c) 2 times and (d) by CVD process.

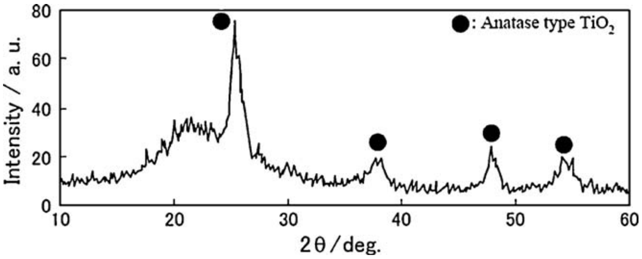

Fig. 8. XRD pattern of porous glass tube supported $TiO_2$ by CVD process.

Fig. 7. CVD process is much more effective than sol–gel process for achieving transparency. XRD measurement, as indicated in Fig. 8, clearly shows the formation of crystalline phase of $TiO_2$ of anatase type. The amount of $TiO_2$ by sol–gel process (impregnation number = 1) is 0.10 g per 1 g of porous glass tube and by CVD process is 0.005 g per 1 g of porous glass tube.

### 3.4. Photooxidation activity

The decomposition rate of the aqueous solution of methylene blue was used as the evaluation of photooxidation activity. The following equation is used to calculate the decomposition rate of methylene blue:

$$\text{The decomposition rate }(\%) = \frac{A_1 - A_2}{A_1} \times 100$$

where $A_1$ is the absorbance of the feed and $A_2$ is the absorbance after photooxidation.

Here, the absorbance is measured at 664 nm.

The contact time ($t$) is calculated by the following equation:

$$t = \frac{SL}{F}$$

where $t$ is the contact time, $S$ is the surface area of the tube ($cm^2$), $L$ is the tube thickness (cm), and $F$ is the flow ($cm^3\ s^{-1}$).

Fig. 9 shows the photooxidation of methylene blue with the concentration of 1 ppm using three types of the tubes. Two of the tubes, (a) and (b), were porous glass tubes B supported $TiO_2$. One was prepared by sol–gel process and the other by CVD process. The tube (c) was an opaque porous alumina tube with 50 nm pore diameter supported $TiO_2$ by sol–gel process. As indicated in Fig. 9, the porous glass tubes show remarkably high photooxidation rate comparing for the opaque porous alumina tube. The porous glass by CVD process shows 90% photooxidation rate at the contact time of 300 s at 1 ppm concentration. However, opaque porous alumina tube supported $TiO_2$ is only 25%. Under these conditions, the porous glass without $TiO_2$ modification was 10%. In order to keep the outer surface area, all the tubes employed here were outer diameter 5 mm and 10 cm long.

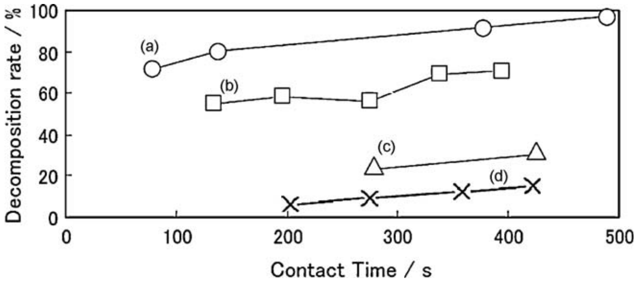

Fig. 9. Decomposition rate vs. contact time for four kinds of tubes: (a) porous glass tube B supported $TiO_2$ by CVD process, (b) porous glass tube B supported $TiO_2$ by sol–gel process (impregnation number = 1), (c) porous alumina tube supported $TiO_2$ by CVD process and (d) porous glass tube B without any modification. Concentration = 1 ppm.

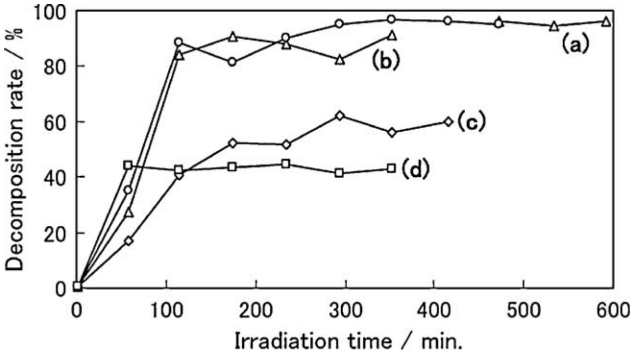

Fig. 10. Decomposition rate vs. irradiation time for aqueous methylene blue solutions with a concentration at (a) 0.4 ppm, (b) 1 ppm, (c) 4 ppm and (d) 10 ppm by porous glass tube B supported $TiO_2$ by CVD process.

By the use of porous glass tube B supported $TiO_2$ with CVD process, Fig. 10 shows the relationship between radiation time and the decomposition rate of methylene blue, which has a concentration from 0.4 to 10 ppm range in an aqueous solution, at the contact time of 300 s. It is clear that the larger the concentration, the smaller the decomposition rate. It takes about 100 min to reach the steady state.

### 3.5. Photoresponse

Fig. 11 shows the photoresponse of porous glass tube supported $TiO_2$ by CVD process at the concentration of 1 ppm and the contact time of 300 s. The asymmetrical photoresponse has a steeper slope for the decomposition rate vs. time in case of lighting on comparing for lighting off. The cause may be considered as follows. The initial $TiO_2$ surface is covered with methylene blue molecules. On lighting on, the molecules on the

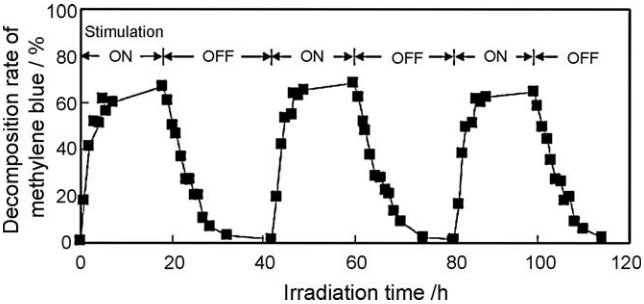

Fig. 11. Light response of the porous glass tube B by CVD process. Concentration = 1 ppm.

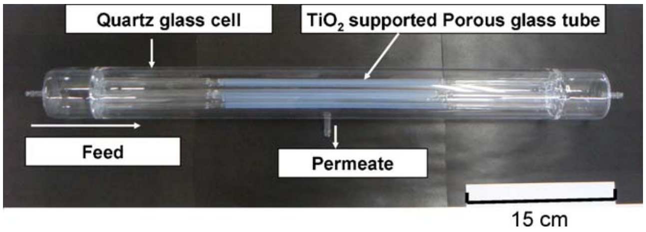

Fig. 12. One example of a reactor composed of the porous glass tube B supported $TiO_2$ by CVD process.

surface are photooxidized and the surface of $TiO_2$ has photooxidation activity. On the other hand, in case of lighting off, the adsorption rate of the molecules on the surface of $TiO_2$ is slower than the decomposition rate of the adsorbed molecules on the surface of $TiO_2$.

Fig. 12 shows one example of photochemical reactor composed of the porous glass tube B supported $TiO_2$ by CVD process.

## 4. Conclusion

A porous glass tube supported $TiO_2$ with high photooxidation activity was obtained. This high photooxidation activity is due to its transparency and large surface area. The most effective process to prepare $TiO_2$ is CVD process, which is reasonable considering that the transparency is maintained during this process. This porous glass tube is widely applicable to photooxidation reactors.

## References

[1] A. Fujishima, T.N. Rao, D.A. Tryk, J. Photochem. Photobiol. C: Photochem. Rev. 1 (2000) 1.
[2] A.L. Linsebigler, G. Lu, J.T. Yates, Chem. Rev. 95 (1995) 735.
[3] M. Yamaguchi, S. Kuriki, P.K. Song, Y. Shigesato, Thin Solid Films 442 (2003) 227.
[4] H. Li, Z. Bian, J. Zhu, Y. Huo, H. Li, Y. Lu, J. Am. Chem. Soc. 129 (2007) 4538.
[5] J.C. Yu, J. Yu, W. Ho, Z. Jiang, L. Zhang, Chem. Mater. 14 (2002) 3808.
[6] E. Vaisman, F.M. Kabir, A. Kantzas, H.C. Labgford, J. Appl. Electrochem. 35 (2005) 675.
[7] T. Moriguchi, M. Tahara, K. Yamaguchi, J. Colloid Interface Sci. 297 (2006) 678.
[8] K. Kata, K. Tsuzuki, A. Taoda, H. Torii, Y. Kato, Y. Butugan, J. Mater. Sci. 29 (1994) 5911.
[9] J. Mullens, M.K. van Bael, H. van den Rul, J. D'haen, J. Sol–Gel Sci. Technol. 14 (1) (2007) 43.
[10] K. Page, R.G. Palgrave, I.P. Parkin, M. Wilson, S.L.P. Savin, A.V. Chadwick, J. Mater. Chem. 17 (1) (2007) 95.
[11] A.I. Kontos, A.G. Kontos, G.D. Vlachos, Thin Solid Films 515 (2007) 7370.
[12] T. Yazawa, F. Machida, K. Oki, A. Mineshige, M. Kobune, Ceram. Int. 35 (2009) 1693.
[13] T. Yazawa, K. Kuraoka, W.-F. Du, J. Phys. Chem. B 103 (1999) 9841.
[14] W.-F. Du, K. Kuraoka, T. Akai, T. Yazawa, J. Phys. Chem. B 105 (2001) 11949.
[15] T. Yazawa, K. Kuraoka, T. Akai, N. Umesaki, W.-F. Du, J. Phys. Chem. B 104 (2000) 2109.
[16] E.P. Barrett, L.G. Joyner, P.P. Halenda, J. Am. Chem. Soc. 73 (1951) 373.
[17] B. Jirgensons, M.E. Straumanis, A Short Textbook of Colloid Chemistry, 2nd ed., Pergamon Press Limited, England, 1962, 98 pp.
[18] P.W. Atkins, Physical Chemistry, 4th ed., Oxford Univ. Press, England, 1990, 1120 pp.